Proc. Budapest'02 Workshop on
Quark & Hadron Dynamics (2002) 000–000

Budapest'02 Workshop on
Quark & Hadron Dynamics
Budapest, Hungary
March 3–7, 2002

Baryon Yields, Isospin Effects and Strangeness Production in Elementary Hadronic Interactions

Hans Gerhard Fischer[1] for the NA49 Collaboration

[1] CERN, CH1211 Geneva 23, Switzerland

Abstract. New NA49 data from hadron + proton and hadron + Pb interactions are used to extract detailed information on projectile isospin effects and baryon, baryon pair and strangeness production. Consequences for the interpretation of hadron production and strangeness enhancement in nuclear collisions are discussed.

Keywords: baryons, isospin, strangeness
PACS: 13.85.Ni

1. Experimental Procedure

The NA49 experiment at the CERN SPS has collected over the past five years at $\sqrt{s} =$ 17.2 GeV sizeable event samples in p + p (2.5 Mevents), π + p (0.8 Mevents), p + Pb (1 Mevents) and π + Pb (0.8 Mevents) interactions. The hadron + Pb data offer centrality control via triggering on grey protons [1] in a range corresponding to 2.5 to 6.5 projectile collisions. Very recently a small (120 kevents) pilot sample of n + p collisions has been obtained. These are derived from d + p reactions by tagging the spectator proton, where the deuterons in turn are produced by fragmentation of a Pb beam in a C target. First studies of meson and baryon production under projectile isospin rotation have thus become feasible. The detector [1] features large acceptance coverage in a range from $x_F = -0.1$ to +0.5 and particle identification via energy loss measurement in the Time Projection Chamber tracking system. Neutrons are measured in a hadronic calorimeter from $x_F = 0.2$ to $x_F = 1$.

2. Isospin Effects in Neutron and Proton Production

The simultaneous measurement of protons and neutrons in p + p and of protons in n + p interactions allows the direct control of isospin symmetry in the $I = 1/2$ baryon doublet as shown in Fig. 1.

If the equality of yields for neutrons from protons and protons from neutrons comes as no surprise in this first experimental verification, it should be noted that the shape and height of the corresponding x_F distributions are not calculable and have to be determined experimentally.

ISBN 963 00 0000 0

Isospin $I = 1/2$		
Projectiles	n	p
Produced particles	n	p
I_3	$-1/2$	$+1/2$

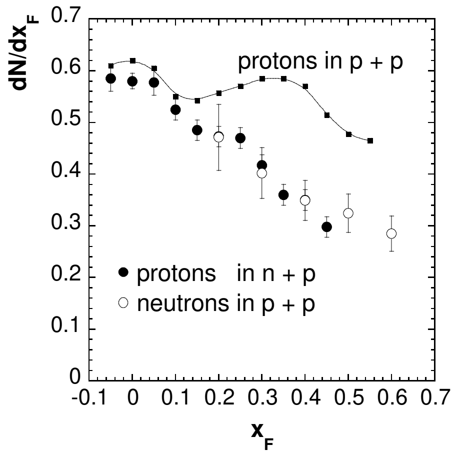

Fig. 1. p_T integrated x_F distributions of protons and neutrons from p + p as well as protons from n + p interactions

The distributions shown in Fig. 1 therefore constitute a basis for the construction of isospin-weighted reference baryon distributions for comparison with interactions of heavy ions which contain typically 60% neutrons. For this comparison it is mandatory to separate out the part of pair produced baryons contributing at low x_F in order to obtain "net" baryon densities. This procedure meets with another range of isospin problems as explained below.

3. Net Baryon Density and Baryon Number Conservation

The sum rule of baryon number conservation in p + p collisions may be written down as follows in the forward hemisphere:

$$\int_{x_F=0}^{1} \left[\frac{dn}{dx_F}(\mathrm{p}-\overline{\mathrm{p}}) + \frac{dn}{dx_F}(\mathrm{n}-\overline{\mathrm{n}}) + \frac{dn}{dx_F}(\mathrm{Y}-\overline{\mathrm{Y}}) + \cdots \right] dx_F = 1.0\,.$$

The difference p – $\overline{\mathrm{p}}$ is usually defined as the number of "net" protons, i.e. the number of leading, non-pair-produced protons. This notion is misleading as pair produced protons may be created together with anti-neutrons and anti-hyperons:

$$\sum(\text{pair-produced protons}) = \mathrm{p}\overline{\mathrm{p}} + \mathrm{p}\overline{\mathrm{n}} + \mathrm{p}\overline{\mathrm{Y}} \cdots\,.$$

A similar sum can be written down for anti-protons:

$$\sum \text{anti-protons} = \overline{\mathrm{p}}\mathrm{p} + \overline{\mathrm{p}}\mathrm{n} + \overline{\mathrm{p}}\mathrm{Y} \cdots\,.$$

The above definition of "net" protons is only valid if either the yield of asymmetric pair production of the type $\mathrm{p}\overline{\mathrm{n}}$ or $\overline{\mathrm{p}}\mathrm{n}$ is zero or if these two terms (to quote only the first contributions) are exactly equal. Both conditions are not fulfilled. A first notion of this problematics may be obtained from Fig. 2 which shows the attempt to obtain "net" proton densities at three cms energies by the subtraction of the $\overline{\mathrm{p}}$ densities from the p densities.

Evidently there remains an instability at $x_F = 0$ in the form of an interference pattern between the shape of the anti-proton distributions and the steeply falling "net" proton distributions which is visible both in the NA49 data and the EHS data at $\sqrt{s} = 27.4$ GeV [2]. At ISR energies [3, 5] this instability develops into a sizeable peak at $x_F = 0$ which, if integrated together with the scaling density distribution at larger x_F, would indicate an increase of the total number of net protons with interaction energy and thereby a problem with baryon number conservation. In order to eliminate these problems the subtraction of more than the measured anti-proton yields seems necessary with a typical increase of around 1.5 in order to obtain "physical" net proton distributions.

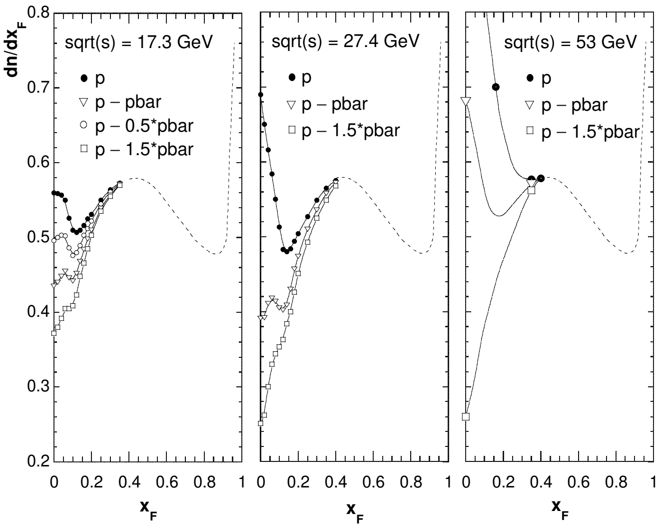

Fig. 2. Net proton distributions as a function of x_F for three cms energies, subtracting different fractions of anti-proton densities from proton densities

4. Anti-Proton Production from Neutron Projectiles

The first ever measurement of anti-proton production from neutron projectiles shown in Fig. 3 quantifies the indications discussed above.

Isospin $I = 1$					
Projectiles		n		p	
Produced particles	$\overline{\mathrm{p}}\mathrm{n}$		$\mathrm{p}\overline{\mathrm{p}}$ $\mathrm{n}\overline{\mathrm{n}}$		$\mathrm{p}\overline{\mathrm{n}}$
I_3	-1	$-1/2$	0	$1/2$	$+1$

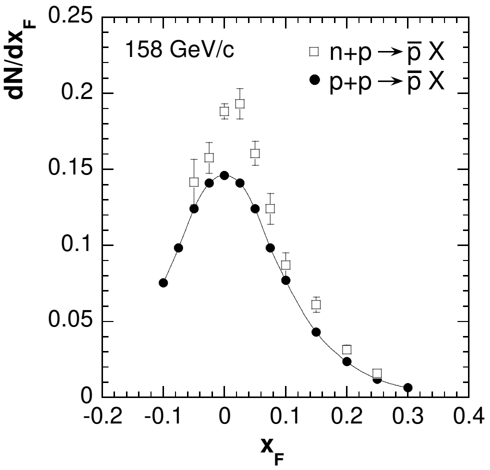

Fig. 3. Anti-proton density distribution as a function of x_F for p + p and n + p interactions

In fact there is a sizeable increase of anti-proton production in n + p collisions if compared to p + p interactions. By making proper allowance for the equal target contribution in both reactions, this increase amounts to a factor of 1.5 to 1.6 at $x_F = 0$. The underlying isospin symmetry may be understood by arranging the possible baryon/anti-baryon combinations evoked in the preceding chapter into the isospin triplet/singlet combinations presented below. The measured yield asymmetry between p and n projectiles corresponds to the preference of the positively charged $\mathrm{p\overline{n}}$ combination over $\mathrm{\overline{p}n}$ with a proton projectile and of the negatively charged $\mathrm{\overline{p}n}$ combination over $\mathrm{p\overline{n}}$ with a neutron projectile. In fact there is a complete correspondence of these isospin states with high mass $I = 1$ mesons with the additional feature that the measurement of $\overline{\mathrm{p}}$ scans both the $I_3 = 0$ (symmetric $\mathrm{p\overline{p}}$) and $I_3 = -1$ (asymmetric $\mathrm{\overline{p}n}$) components. The observed sizeable increase factor therefore corresponds to a very strong asymmetric component.

5. Consequences for Central Net Baryon Density

The evolution of the invariant p_T-integrated proton and anti-proton cross sections at $x_F = 0$ with $\sqrt{s}$ is presented in Fig. 4a for p + p collisions. A sharp decrease of central proton density up to $\sqrt{s} \simeq 20$ GeV is followed by a minimum at around 25 GeV and an increase at higher energies which traces the development of the anti-proton cross section. If subtracting the anti-proton from the proton yield the invariant "net" proton density reaches a constant level above $\sqrt{s} \simeq 30$ GeV (see Fig. 4b) which illustrates again the problem with baryon number conservation mentioned above, as a constant invariant cross section at $x_F = 0$ implies a central proton density which increases linearly with $\sqrt{s}$.

If, however, a larger amount of anti-protons is subtracted (in Fig. 4b, 1.6 times the measured yield) the "net" proton cross section approaches zero in the upper ISR energy range thus precluding a divergence of total proton number.

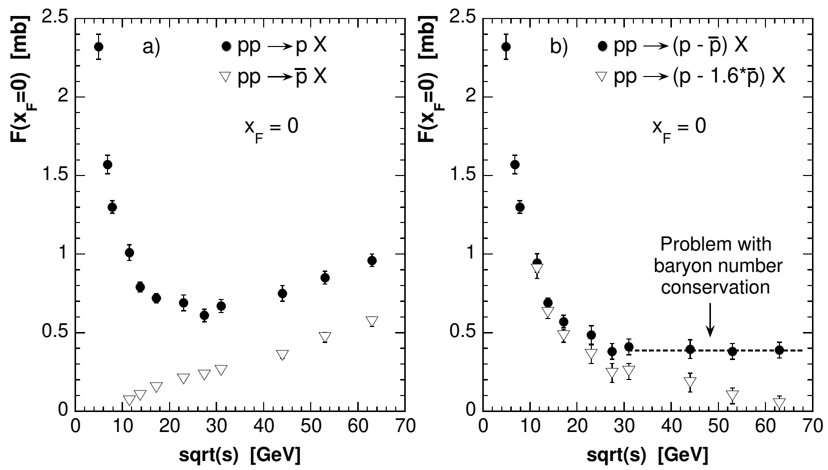

Fig. 4. a) p_T-integrated invariant p and $\overline{\mathrm{p}}$ yields at $x_F = 0$ as a function of $\sqrt{s}$ b) p – $\overline{\mathrm{p}}$ and p – 1.6 $\cdot\,\overline{\mathrm{p}}$ as a function of $\sqrt{s}$

6. Consequences for Hyperon Yields

The observed pattern of isospin dependencies for baryons may be extended to strange and double-strange hyperons noting the following isospin multiplets (making no difference in notation between Λ^0 and Σ^0 which are anyway indistinguishable in most experiments):

Isospin $I = 1$						Strangeness
Projectiles		n		p		
Produced particles	$\Lambda\overline{\Sigma}^-$ $\Sigma^-\overline{\Lambda}$		$\Lambda\overline{\Lambda}$		$\Lambda\overline{\Sigma}^+$ $\Sigma^+\overline{\Lambda}$	$-1, +1$
I_3	-1	$-1/2$	0	$1/2$	$+1$	

Isospin $I = 1$						Strangeness
Projectiles		n		p		
Produced particles	$\overline{\Xi}^0\,\Xi^-$		$\Xi^0\overline{\Xi}^0$ $\Xi^-\overline{\Xi}^+$		$\Xi^0\overline{\Xi}^+$	$-2, +2$
I_3	-1	$-1/2$	0	$1/2$	$+1$	

As a consequence of the possible combination of $I_3 = 0$ states (Λ^0, Σ^0) with $I_3 = \pm 1$ states ($\Sigma^\pm$) it is apparent that there should be no dependence of Λ^0 and $\overline{\Lambda}^0$ yields on projectile charge. In other words the $\overline{\Lambda}^0$ measures the total number of pair produced Lambda's and the quantity $\Lambda^0 - \overline{\Lambda}^0$ gives the yield of "net" Lambda hyperons. This is visible in Fig. 5 where the s-dependence of invariant Λ^0 and $\overline{\Lambda}^0$ yields are given at $x_F = 0$. Within the sizeable error bars several basic features are noteworthy:

a) The rapid decrease of net hyperon number up to $\sqrt{s} \simeq 20$ GeV followed by a minimum at $\simeq 25$ GeV and an increase which traces the evolution of the $\overline{\Lambda}^0$ yield from a threshold at $\simeq 7$ GeV (see Fig. 4a for comparison).

b) The steep decrease of net hyperon number below $\sqrt{s} \simeq 8$ GeV corresponding to the threshold cut-off in associate (Λ, K) production.

c) The much smaller difference between Λ^0 and $\overline{\Lambda}^0$ yields at $\sqrt{s}$ around and above 25 GeV if compared to p and $\overline{\mathrm{p}}$ (Fig. 4). This leads to a rapid decrease of the "net" Λ^0 yield with $\sqrt{s}$ at ISR energies.

Concerning the cascade baryons and anti-baryons, their isospin triplet is in complete charge-antisymmetry to the triplet of protons and anti-protons. Therefore the number of pair produced Ξ^- is smaller than the number of $\overline{\Xi}^+$ in p + p interactions in opposition to the case of pair produced protons and anti-protons. Consequently in passing to neutron-induced in-

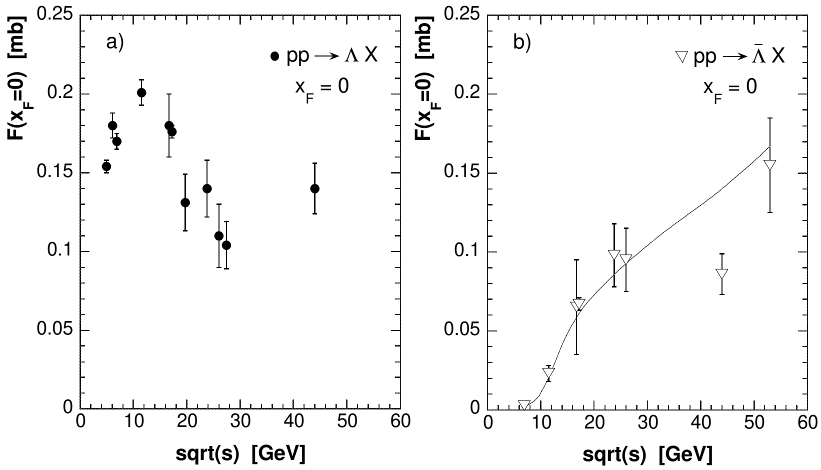

Fig. 5. p_T-integrated invariant cross sections at $x_F = 0$ for a) Lambda and b) Anti-Lambda as a function of $\sqrt{s}$. The line in b) gives the scaled s dependence of anti-protons.

teractions one should predict an increase of Ξ^- and a decrease of $\overline{\Xi}^+$ yields with important consequences for the interpretation of the enhanced production of these particles in $A + A$ collisions. Proceeding to Ω-hyperon production NA49 has obtained a first clear signal of

Ω^- in p + p interactions whereas there is — with the present event statistics — no $\overline{\Omega}^+$ visible. Nevertheless this allows to establish an upper limit of the $\overline{\Omega}^+ / \Omega^-$ ratio of 0.5 with 95% confidence level. The combined situation of anti-baryon/baryon ratios as a function of strangeness content is given in Fig. 6.

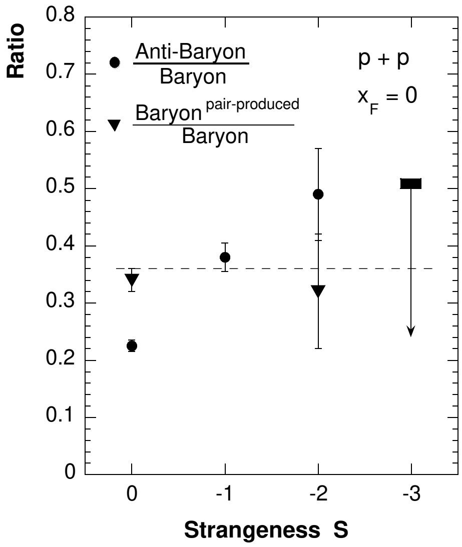

Fig. 6. Anti-baryon/baryon and pair-produced-baryon/baryon ratios at $x_F = 0$ in p + p interactions as a function of strangeness content

The apparent increase of this ratio with strangeness content can, based on the above discussion, be traced to isospin effects which have to and can be corrected for. This leads to the redefinition of the ratio as pair-produced-baryons/baryons. If applying the measured isospin correction to anti-protons and the predicted (and opposite) correction to $\overline{\Xi}^+$ one obtains within error bars a flat dependence of this redefined ratio on strangeness as indicated in Fig. 6.

7. Comparison of Cascade Baryon Production in p + p, p + Pb and Pb + Pb collisions

In the following the problems of comparison between different hadronic processes, of isospin effects and of the interpretation of "enhancement" effects will be exemplified for the case of cascade baryon production.

Measurements of cascade baryon cross sections are available from the WA97 [6] and NA49 [7] experiments at the SPS and are given in Table 1. These measurements fortunately enough cover a wide range of hadronic interactions with a welcome overlap which allows control of consistency. The table also contains two very important normalization and reference numbers: the number of "wounded nucleons" NW and the number of collisions ν per projectile nucleon characterizing each reaction.

Table 1. See text

	pp	pBe	pPb	pPb	pPb	PbPb	PbPb
	NA49	WA97	WA97	NA49	NA49	WA97	NA49
NW	2	2.5	4.7	4.7	6.7	350	362
ν	1	1.5	3.7	3.7	5.7	4.5	4.5
Ξ^-	0.00074	0.0015	0.003	0.004	0.0058	1.5	1.49
$\overline{\Xi}^+$	0.00036	0.00068	0.0012	0.0014	0.0018	0.37	0.33

7.1. *Comparison of Pb + Pb and p + p interactions*

Dividing the cascade yields in Pb + Pb collisions by the number of participant pairs (equal NW/2) one obtains, now seen per participant pair collision, and averaging over the NA49 and WA97 results (which agree within their 15% error limits) the following central rapidity densities:

			isospin corrected	
	Ξ	$\overline{\Xi}$	Ξ	$\overline{\Xi}$
p + p	0.00074	0.00036	0.00096	0.00028
Pb + Pb	0.0082	0.0019		
PbPb/pp	11.0	5.3	8.54	6.8

The above ratios constitute a) a very sizeable cascade baryon enhancement and b) a difference of a factor of two in enhancement between baryon and anti-baryon. The difference in isospin composition between p + p and Pb + Pb collisions should however, as discussed in Section 6 above, be taken into account. It has been shown that one has, at least for Ξ pair production, to expect a decrease in $\overline{\Xi}$ and an increase in Ξ yield when switching from p to n projectile. Assuming this isospin effect to be of the same order as the one for protons/anti-protons quantified in Section 5 as about 1.5, the resulting net correction factor for the elementary nucleon + nucleon collision would be $(0.6 \cdot 1.5 + 0.4 \cdot 1.0) = 1.3$. The application of this correction changes the enhancement of Ξ^- and $\overline{\Xi}^+$ to 8.5 and 6.8, respectively. As a consequence, the difference in baryon and anti-baryon enhancements is drastically reduced.

It should be clear from this example that the measurement of Ξ and $\overline{\Xi}$ cross sections in both p + p and n + p collisions is absolutely necessary for argumentations about the excess of cascade production in $A + A$ reactions.

7.2. *Comparison of p + A and p + p interactions*

Contrary to the symmetric nucleon + nucleon and nucleus + nucleus interactions discussed above, the hadron + nucleus collisions are by construction asymmetric. At a given impact parameter the projectile hadron will hit ν target nucleons (see Table 1 above). The projectile fragmentation will thus be characterized by hadronization after multiple collisions, as is the case for *all* participating nucleons in a nucleus + nucleus interaction. The “wounded” target nucleons in a p + A reaction on the contrary are only hit once and are therefore — in their fragmentation — characterized by single collision physics i.e. close to the elementary nucleon + nucleon interaction. The final state hadron density will therefore have two components: a target component which is the approximate sum of ν elementary hadronization processes and a projectile component which carries the imprint of multiple (ν) collisions. Only the latter component should be comparable to nucleus + nucleus interactions.

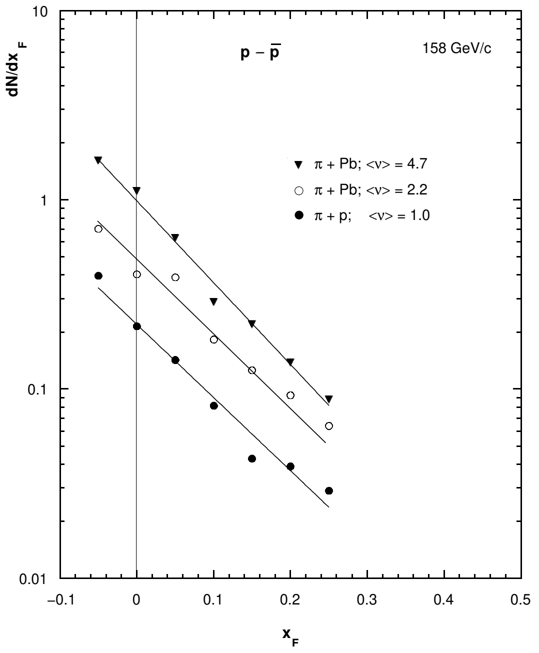

Fig. 7. p – $\overline{\mathrm{p}}$ yield as function of x_F for π + Pb interactions at different centralities, i.e. different mean number of collisions $\langle\nu\rangle$, and π + p collisions ($\langle\nu\rangle = 1$)

The NA49 experiment has been able to check the superposition argument evoked above for the target component in the specific case of net baryon production in p + Pb collisions. Using data from both π^+ + Pb and π^- + Pb interactions which have no “net” baryon content on the projectile level (see also argumentation concerning π^+ + p and π^- + p in Section 5 above) one can use the quantity p – $\overline{\mathrm{p}}$ in order to measure directly the evolution of target baryon density with the number nu of collisions. The result of this measurement is given in Fig. 7. Here the net proton density is plotted as a function of x_F for p + p collisions and average π + Pb collisions at two different impact parameters corresponding to 2.2 and 4.7 projectile collisions. The approximate linearity of yield against ν at $x_F = 0$ is evident. This observation allows to set up a simple superposition formula for particle yields at $x_F = 0$ in p + A collisions:

$$(dn/dx)^{\mathrm{p}+A}_{x_F=0} = (dn/dx)^{\mathrm{p+p}}_{x_F=0} \cdot (0.5 \cdot (\nu \cdot \alpha) + 0.5 \cdot E),$$

where the “enhancement factor” E describes the deviation of the projectile component (multiple collisions) from the simple p + p behaviour (single collision) and the parameter α the influence of isospin effects on particle yield due to the composition of A from by protons and neutrons.

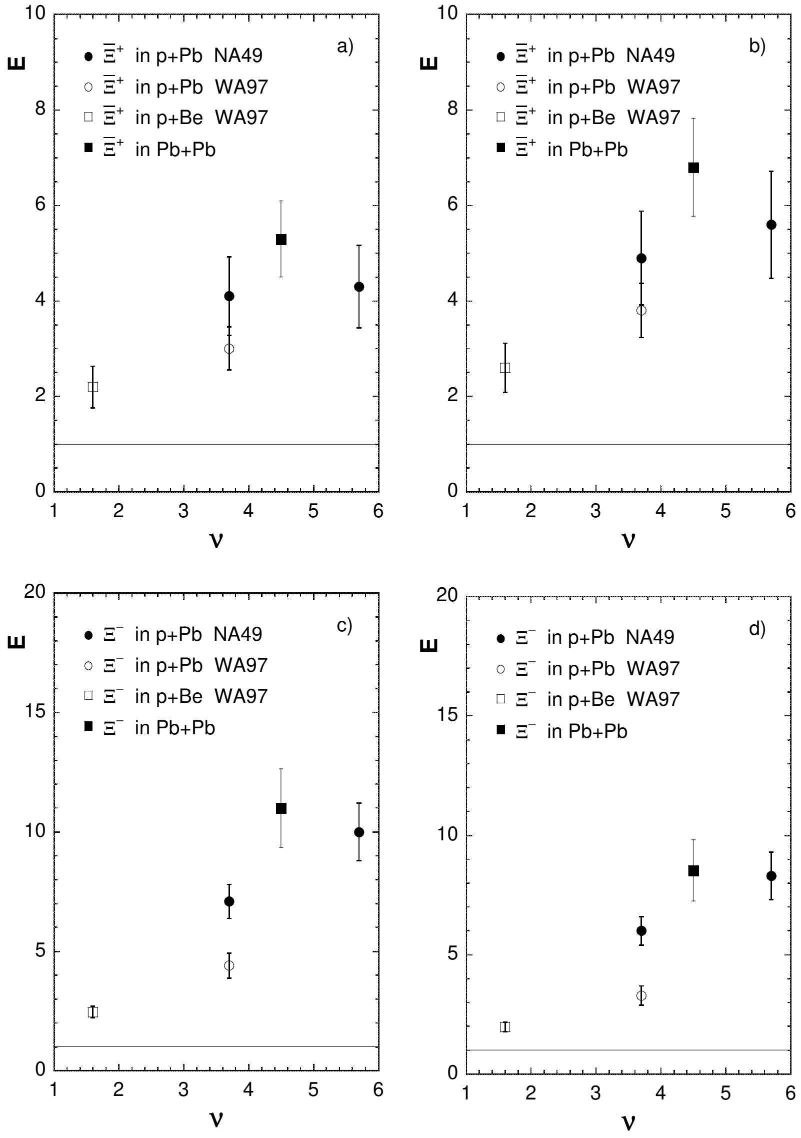

Fig. 8. Enhancement factor for the production of a) Ξ^+ and c) Ξ^- as measured and b), d) taking into account the isospin correction deduced from p and $\overline{\text{p}}$ yields of p + p and n + p collisions.

This formula demonstrates clearly that with increasing number of collisions the relative weight between target "pile-up" and projectile fragmentation becomes bigger and bigger contrary to $A+A$ collisions where this formula should read:

$$(dn/dx)^{A+A}_{x_F=0} = (dn/dx)^{N+N}_{x_F=0} \cdot (0.5 \cdot E + 0.5 \cdot E) \cdot NW/2\,.$$

The visibility of any enhancement effect due to multiple collisions is therefore strongly suppressed in p + A in comparison to $A+A$ collisions for central x_F (see argumentation in Section 8.2 for kaon production).

By applying the above formalism the cascade baryon measurements of table 1 in p + A interactions can now be confronted with both the elementary p + p and the multi-collision Pb + Pb results and the enhancement factors E extracted from the data, see Fig. 8. From this figure two conclusions may be drawn:

a) With or without taking into account isospin effects the cascade yields measured in Pb + Pb collisions comply within experimental errors with the ν dependence extracted from p + p and p + Pb interactions.

b) The application of isospin effects of the expected order of magnitude reduces the difference between $\overline{\Xi}^+$ and Ξ^- enhancements both in p + Pb and Pb + Pb reactions.

Both findings agree with what has been concluded in Section 8.2 for K meson production.

It is clear that — in order to replace conjecture by reality as far as isospin effects are concerned — the measurement of $\overline{\Xi}^+$ and Ξ^- with neutron beam is a necessity.

8. Isospin Effects in Mesonic Production

8.1. Results on charged pions

Projectiles		n	p
Produced particles	π^-	π^0	π^+
Isospin	-1	0	$+1$

The expected ("trivial") isospin symmetry in pion production i.e. the complete flip between π^+ and π^- yields when changing from proton to neutron projectile has not been measured to any precision in the SPS energy range. Results as a function of transverse momentum at fixed x_F are presented in Fig. 9 which shows that indeed charge reflection symmetry is achieved within statistical errors of a few percent over a wide range of p_T. This is extended to a wider x_F interval in Fig. 10 which shows p_T-integrated π^+/π^-, resp. π^-/π^+ ratios as a function of x_F. Here two regions are of interest:

a) At low x_F, π^-/π^+ should approach 1 in n + p interactions if charge reflection holds. This is borne out by the measurements shown in Fig. 10. The extent of the transition region in x_F offers a first determination of pion feed-over from target to projectile

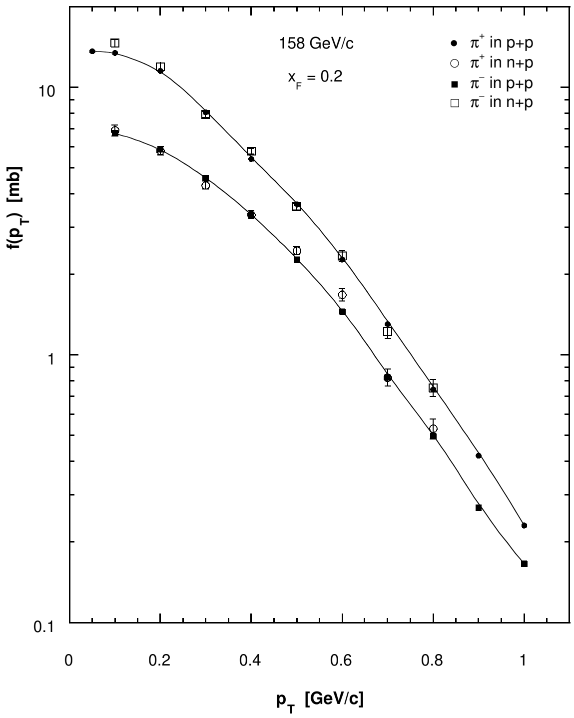

Fig. 9. Differential invariant cross section as function of p_T at $x_F = 0.2$ for π^+ and π^- produced in p + p and n + p interactions

hemisphere. It is visible that the feed-over is small already at $x_F = 0.05$ and vanishes at about $x_F = 0.1$. This result is important for some of the conclusions drawn below.

b) At large x_F, the pionic charge ratios become large and therefore allow a more sensitive test of charge reflection symmetry which is not a priori implied by isospin invariance. The present data (see Fig. 10) cannot exclude such effects and it would be desirable to obtain similar statistical errors in n + p and p + p reactions.

8.2. Results on charged kaons

Due to strangeness conservation the situation is more complex for strange meson production. In fact kaons may be produced

a) in conjunction with hyperons ("associate production") and

b) in pairs.

Mechanism a) can be described by the isospin quadruplet shown in the table below. As in this process the s-quark is fixed in the hyperon, the K^+ yield ($\bar{s}$-quark) will not commute with the K^- yield (s-quark). K^- can only be produced here in the decay of Y^* (Σ^*) resonances which also yield $\overline{K}^0$. Consequently, in the "associate" hyperon–kaon

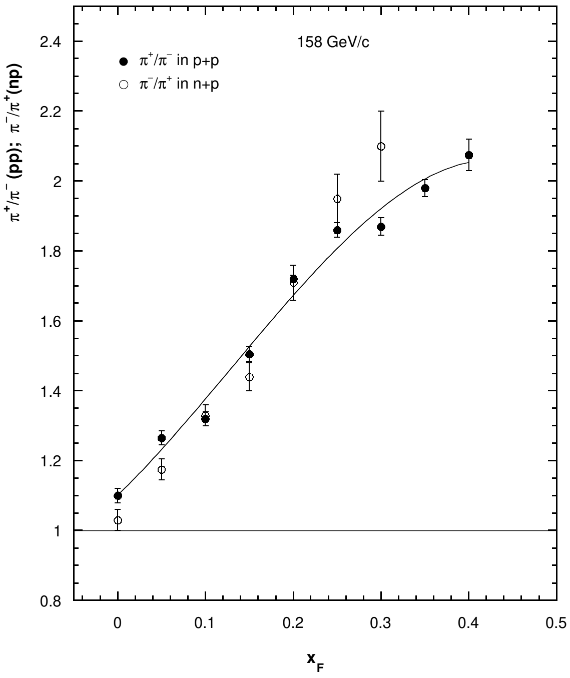

Fig. 10. π^+/π^- ratio in p + p and π^-/π^+ ratio in n + p interactions as function of x_F

			Strangeness
Projectiles	n	p	
Produced particles	K^0	K^+	1
	K^-	$\overline{K}^0$	−1
Isospin	−1/2	+1/2	

channel, by exchanging p with n projectile, instead of $K^+ \leftrightarrow K^-$ the commutation $K^0 \leftrightarrow K^+$ and $\overline{K}^0 \leftrightarrow K^-$ should be dominant. This argument also raises questions about the isospin dependence of K^0_s production which "bridges" the multiplet by having both K^0 and $\overline{K}^0$ content.

The kaon pair production mechanism (b) corresponds to the isospin triplet, shown in the table below. In this case — and in analogy with the pion triplet discussed in the preceding section — one has to expect a definite dependence of charged kaon production on projectile charge: K^+ production should be reduced, K^- production enhanced when switching from p to n projectile. The relative weight of mechanisms a) and b) in charged kaon production is not predicted from soft QCD. It can be expected, though, that process a) should dominate in the threshold region at low cms energy, whereas process b) should become more and more important as energy increases.

				Strangeness
Projectiles		n	p	
Produced particles	K^-K^0	K^+K^- $K^0\overline{K}^0$	$K^+\overline{K}^0$	0
Isospin	-1		1	

NA49 has obtained the first comparative measurement of charged kaons with both p and n beams. Fig. 11 shows kaon yields as a function of p_T at two values of x_F in the projectile region. It is apparent that compared to the charged pions the charged kaons *do not*

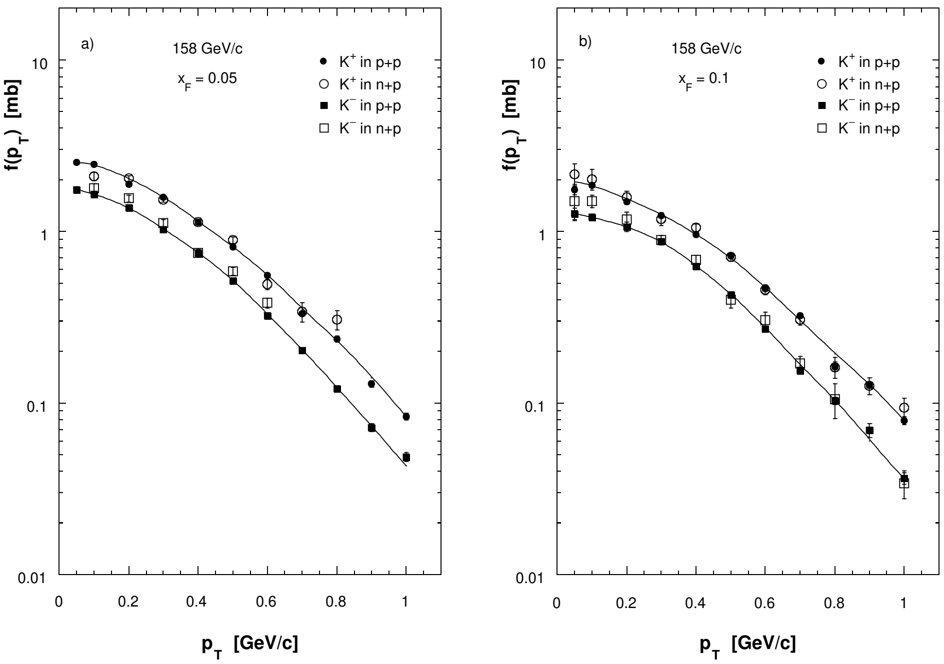

Fig. 11. Differential invariant cross section as function of p_T at a) $x_F = 0.05$ b) $x_F = 0.1$ for K^+ and K^- produced in p + p and n + p interactions.

commute with projectile isospin. Within statistical errors on the contrary, both K^+ and K^- yield are invariant against projectile charge. This observation carries strong consequences for K/π ratios as shown in Fig. 12 for K^+/π^+ and K^-/π^- from protons and neutrons as a function of x_F. Interpretation of K/π ratios from nuclei and their comparison to p + p interactions has therefore to take account of the proper isospin mixture in these nuclei. The necessary correction factors for Pb + Pb collisions are shown in Fig. 13: they reach (at

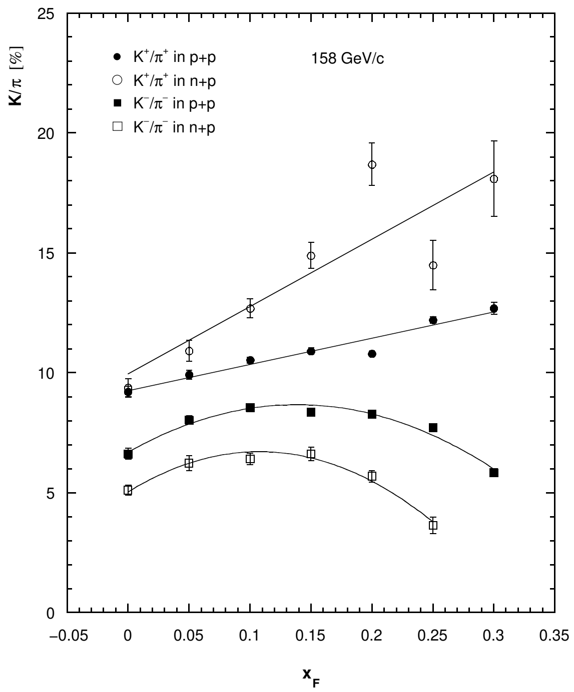

Fig. 12. K^+/π^+ and K^-/π^- ratio as function of x_F in p + p and n + p interactions

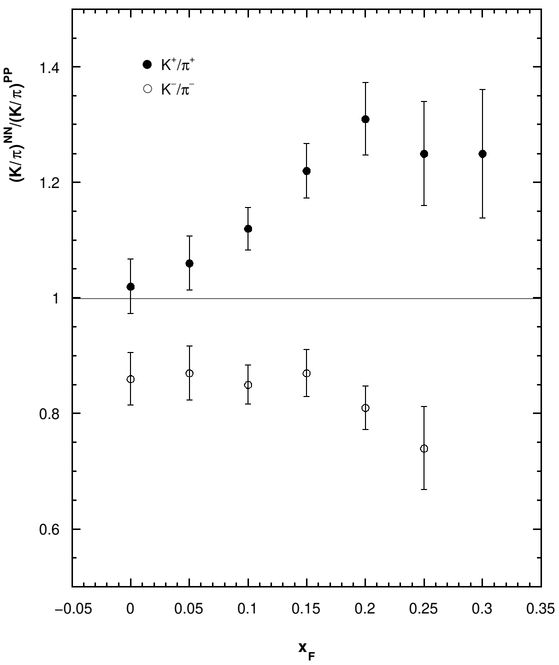

Fig. 13. Ratios $(K^+/\pi^+)^{NN}/(K^+/\pi^+)^{pp}$ and $(K^-/\pi^-)^{NN}/(K^-/\pi^-)^{pp}$ as function of x_F representing the correction factors to be applied when comparing Pb + Pb and p + p interactions in order to account for the proper isospin composition of the Pb nucleus (60% n projectiles and 40% p projectiles)

158 AGeV) values of up to 30%, depending on x_F. This is exemplified in Fig. 14 where K^+/π^+ and K^-/π^- ratios from Pb + Pb collisions as measured by NA49 are presented both uncorrected and corrected for isospin effects. NA49 has also obtained K/π ratios from p

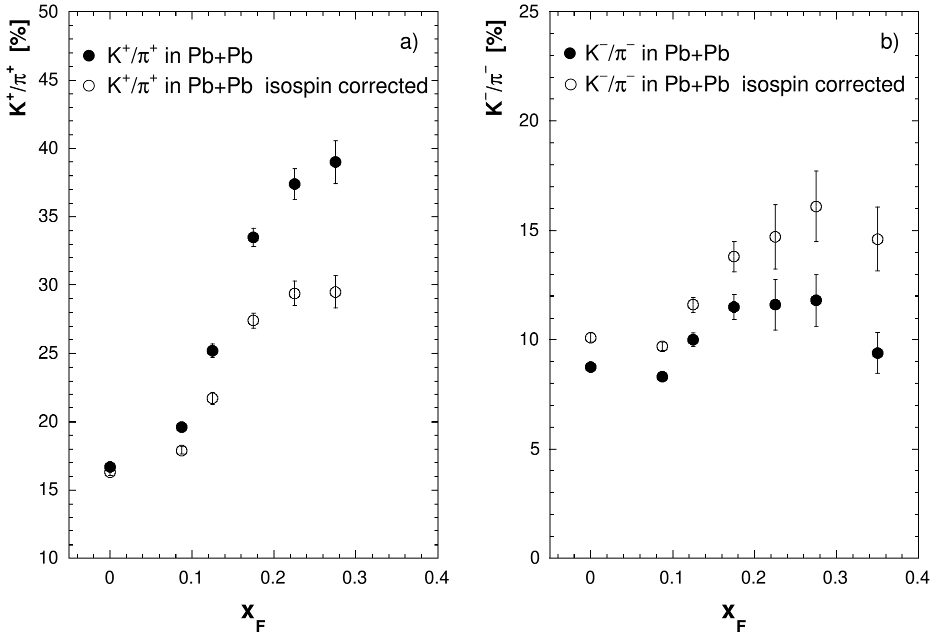

Fig. 14. a) K^+/π^+ ratio b) K^-/π^- ratio as function of x_F for Pb + Pb collisions as measured and taking into account the proper isospin composition of the Pb nucleus (60% n projectiles and 40% p projectiles).

+ Pb interactions with controlled centrality. Here the comparison to the elementary p + p collisions is straight-forward in the p projectile hemisphere, but suffers from isospin effects in the backward (Pb) hemisphere. In the transition region around $x_F = 0$, in addition target-pile-up in this multiple collision process has to be taken into account, as described above in Section 7.

Target feed-over effects are expected to reach out to about $x_F = 0.05$ (see above) and can be corrected for by using the approximate linearity of target yields with the number of collisions.

The thus corrected K/π ratios are compared to Pb + Pb interactions in Fig. 15.

Apparently, both for K^+ and K^- ratios there is — within statistical erors — *no difference* visible between both types of reactions, and this over the complete x_F range accessible to NA49. This constitutes an important result for the interpretation of $A + A$ collisions.

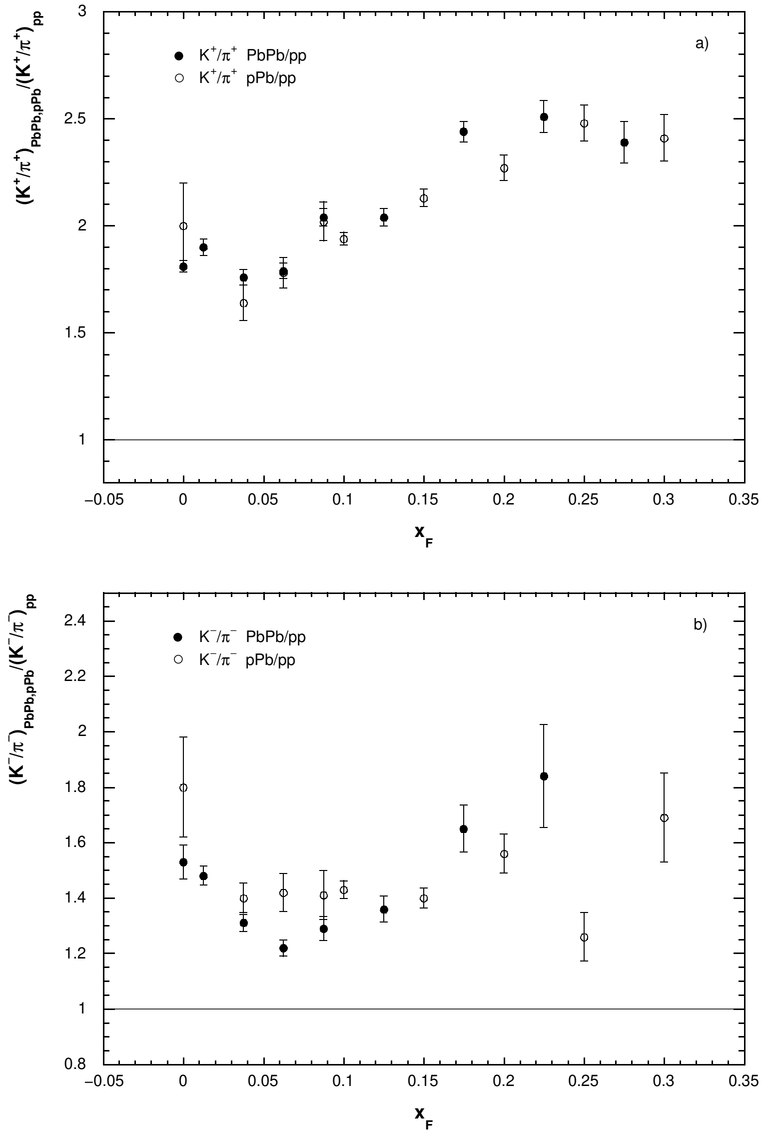

Fig. 15. a) K^+/π^+ ratio b) K^-/π^- ratio as function of x_F for p + Pb and isospin corrected Pb + Pb collisions normalized to p + p interactions

9. Conclusions

New data from the CERN SPS concerning projectile isospin rotation and baryon, meson and strangeness production in elementary hadronic interactions have been discussed. Their exploitation offers improved insight into the detailed mechanisms of isospin symmetry, baryon number transfer, the evolution of net baryon density, and mesonic and baryonic strangeness production. Comparisons to the more complex hadron + nucleus and nucleus + nucleus collisions demonstrate the importance of such studies for a more precise interpretation of nuclear effects.

Notes

a. Permanent address: CERN, Geneva, Switzerland;
E-mail: Hans.Gerhard.Fischer@cern.ch

References

1. S. Afanasiev et al., *Nucl. Instr. Meth.* **A430** (1990) 210.
2. M. Aguilar-Benitez et al. (NA27 Collaboration), *Z. Phys.* **C50** (1991) 405.
3. K. Guettler et al., *Nucl. Phys.* **B116** (1976) 77.
4. Note concerning Ref. [2] and [3]: as the ISR data are not corrected for hyperon feed-down this correction (using data of Fig. 5 plus an assumption on the Σ-yield) has been performed to obtain the values shown in Fig. 4.
5. B. Alper et al., *Nucl. Phys.* **B100** (1975) 237.
6. F. Antinori et al. (WA97 Collaboration), *Nucl. Phys.* **A661** (1999) 130c.
7. T. Susa et al. (NA49 Collaboration), *Nucl. Phys.* **A698** (2002) 491c.